

Environmental Science Processes & Impacts

Accepted Manuscript



This is an *Accepted Manuscript*, which has been through the Royal Society of Chemistry peer review process and has been accepted for publication.

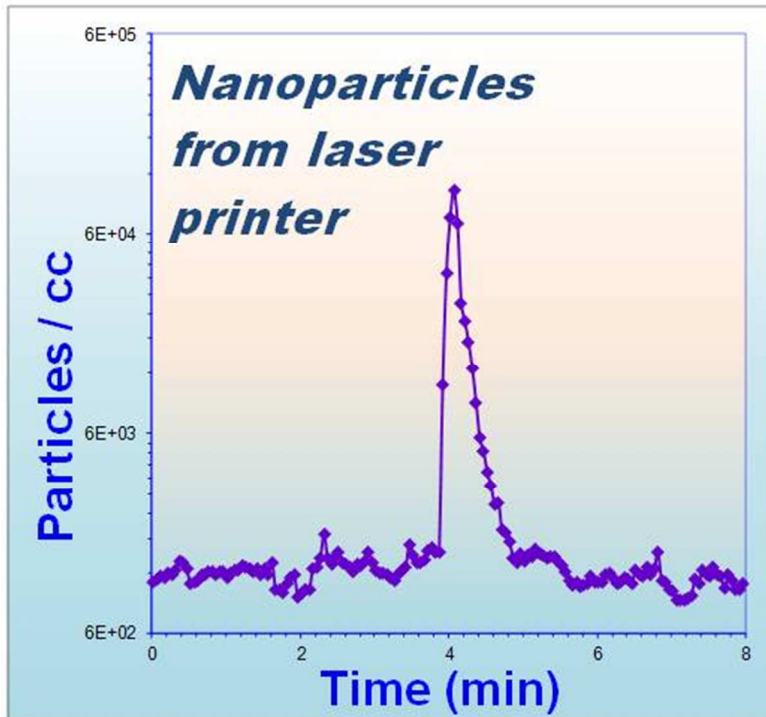
Accepted Manuscripts are published online shortly after acceptance, before technical editing, formatting and proof reading. Using this free service, authors can make their results available to the community, in citable form, before we publish the edited article. We will replace this *Accepted Manuscript* with the edited and formatted *Advance Article* as soon as it is available.

You can find more information about *Accepted Manuscripts* in the [Information for Authors](#).

Please note that technical editing may introduce minor changes to the text and/or graphics, which may alter content. The journal's standard [Terms & Conditions](#) and the [Ethical guidelines](#) still apply. In no event shall the Royal Society of Chemistry be held responsible for any errors or omissions in this *Accepted Manuscript* or any consequences arising from the use of any information it contains.



rsc.li/process-impacts



Characterization of incidental nanoparticles (such as diesel fumes and printer emissions) is an important component of nanotechnology exposure assessments.

An important component of assessing exposure to engineered nanoparticles is characterization of background. Quantification of engineered nanomaterial exposure can be very challenging due to temporal and spatial variability of incidental nanoparticles. In this study particle size distribution, particle count, and particle surface area are monitored in six locations of an indoor workplace environment, where incidental nanoparticles are found to be the largest contributor to the background aerosol. Strong temporal trends, i.e. a clear increase or decrease in background nanoparticles, are observed in several locations, demonstrating the importance of including time series data in an exposure assessment. The study concludes that the most appropriate measurement strategy is situation specific, and should include multiple direct-reading instruments to cover all the relevant measurands.

Spatial and temporal variability of incidental nanoparticles in indoor workplaces: impact on the characterization of point source exposures

Jianjun Niu^a, Pat E. Rasmussen^{a,b,δ}, Robert Magee^c, Gregory Nilsson^c

^a*Environmental Health Science and Research Bureau, HECSB, Health Canada, Ottawa, Ontario, Canada K1A 0K9*

^b*Earth Sciences Department, University of Ottawa, Ottawa, Ontario, Canada K1N 6N5*

^c*National Research Council of Canada, Intelligent Building Operations, 1200 Montreal Road, Ottawa, Ontario, Canada K1A 0R6*

Abstract

This study deployed a suite of direct-reading instruments in six locations inside one building to characterize variability of the background aerosol, including incidental nanoparticles (NP), over a six month period. The instrument suite consisted of a portable Condensation Particle Counter (CPC) and a Scanning Mobility Particle Sizer (SMPS) for assessing particle number concentrations and size distributions in the nano-scale range; an Aerodynamic Particle Sizer (APS) for assessing micron-scale particle number concentrations and size distributions; plus a desktop Aerosol Monitor (DustTrak DRX) and a Diffusion Charger (DC2000CE) for assessing total particle mass and surface area concentrations respectively. In terms of number concentration, NPs (<100 nm) were the dominant particles observed in the background aerosol, contributing up to 53% -93% of the total particle number concentrations. The particle size distributions were bimodal with maxima around 19-79 nm and 50-136 nm, respectively, depending on workplace locations. The average detected background particle number, surface area and total mass concentrations were below $7.1 \times 10^3 \text{ \# cm}^{-3}$, $22.9 \text{ \mu m}^2 \text{ cm}^{-3}$ and $33.5 \text{ \mu g m}^{-3}$, respectively in spring samples and below $1.8 \times 10^3 \text{ \# cm}^{-3}$, $10.1 \text{ \mu m}^2 \text{ cm}^{-3}$ and $12.0 \text{ \mu g m}^{-3}$, respectively in winter samples. A point source study using an older model laser printer as the emission source indicated that NPs emitted from the investigated printer were distinguishable from background. However, more recent low emitting printers are likely to be indistinguishable from background, and chemical characterization (e.g. VOCs, metals) would be required to help identify emission sources.

Keywords: *Nanoparticle exposure, workplace, indoor air, background characterization, ultrafine particles, surface area, mass, particle size distribution.*

^δ *Corresponding author: Tel: (613)941-9868, fax: (613)952-8133.
e-mail: Pat.Rasmussen@hc-sc.gc.ca*

1. Introduction

An important but challenging aspect of characterizing nanoparticle (NP) exposures in the workplace is the necessity to quantify background or “incidental” NPs [1-3]. The term nanoparticle originally referred to engineered nanoparticles but is now defined as any particle less than 100 nm in three dimensions [4], which includes ultrafine particles (UFPs) that originate from multiple incidental sources in indoor environments including office electronic equipment, cosmetics, food and packaging, clothing and textiles, heating and cooking [5-8] and infiltration from outdoor sources such as combustion and vehicle emissions [7,9,10]. Appropriate characterization of background NPs is a critical step to avoid misidentification of exposure sources [11-13] but currently there is limited guidance for measurement and characterization of background NPs and for differentiating background from engineered NP exposure in the workplace [14-16]. Background NP concentrations may vary widely depending on the unique conditions of the workplace [17, 18], and thus it may be difficult or impractical to correct for background using a simple subtraction approach. Background correction to identify point-source contributions of NP becomes quite complex if the investigated source contributes relatively small elevations in particle counts while the background particle count is relatively high [18].

There is also a lack of international consensus about which measurement parameters (solubility, size, surface area, morphology, composition, degree of agglomeration/aggregation, surface modifications or reactivity, number concentration, and/or mass) provide the most reliable exposure metrics [2,17,19,20]. Animal studies have indicated

that the toxicity of inhaled NPs or UFPs is more closely associated with particle surface area and particle number concentrations than with the particle mass concentration when comparing aerosols having different particle size distributions [21-23]. However, mass concentration measurements are still considered valuable and necessary in many situations [3]. For this reason, it has been recommended that several different exposure metrics should be captured (e.g., particle number concentration, surface area concentration, and mass concentration) which requires the use of multiple instruments operated simultaneously [17-20, 24-29]. If source identification is required, NPs may need to be sampled for off-line chemical and physical characterization using techniques such as inductively coupled plasma-mass spectrometry (ICP-MS), energy dispersive X-ray fluorescence (ED-XRF), atomic force microscopy (AFM), electron microscopy (EM), and X-ray diffraction (XRD) [9,13,30-33].

The present paper is organized into two parts: a Background Study and a Point Source Study. The main focus of the Background Study is the investigation of spatial and temporal variability of indoor background aerosols using key parameters: particle number concentrations, total surface area and mass concentrations, and particle number and mass size distributions. This study was carried out at different locations and times in a single federal workplace building as a preliminary characterization of incidental (background) nano-sized particles. The Point Source Study focuses on assessing the capacity of the instrument suite to measure and distinguish a known point source of NP emissions (compared to background) in a workplace environment. Laser printers, which are a very common point source of NP emissions [5,17,34-36], were used in this study to assess the analytical ability to discriminate these point sources from background levels in each of

the six investigated locations. In addition to NPs, the fine and coarse particle size ranges (100 nm - 20000 nm) were also monitored using both research grade instruments and analyzers traditionally used by occupational hygienists for characterization of aerosol trends.

2. Experimental

2.1. Background study

2.1.1. Study design

The purpose of the background study was to obtain a preliminary set of background aerosol measurements that will assist in determining appropriate monitoring approaches to characterize background NPs as part of future occupational health and safety exposure assessments for work involving engineered nanomaterials. These background measurements are the first step in an exposure assessment program aimed at monitoring airborne engineered nanomaterials. The background study was performed at six locations on the ground floor of a single federal government building in Ottawa, Ontario, Canada. There was no handling or use of engineered nanomaterials during this study.

The suite of instruments listed in Table 1 was set up on carts for simultaneous direct monitoring of the key parameters. A limitation of the background study was the availability of only one complete suite of instruments, due to the total combined cost of these instruments. Therefore the six locations could not be monitored simultaneously as it was necessary to move the instrument suite consecutively from one location to another.

Continuous monitoring was conducted for a 3-4 day period in each location, from which a 24 hr subset was extracted based on time stamps (midnight to midnight) to allow comparisons of 24 hr averages and standard deviations. The criteria for selection of the 24 hr subsets were (1) presence of a complete data set for all instruments, and (2) minimal human activity during monitoring to avoid disrupting the suite of instruments. Apart from the single operator of the instrument suite, there were no other occupants present in the four investigated rooms, but human activity was not controlled in the corridor (20-50 passers-by during the day/2-4 at night or the receiving/delivery area (5-15 deliveries per day/none at night). The 24 hr subsets were further divided to obtain 12 hr daytime averages (6:30 am - 6:30 pm) and 12 hr nighttime averages (6:30 pm - 6:30 am).

Measurements were taken twice in each location: once in the winter (November 2011 to January 2012) and once in the spring (April to May 2012). Although the resulting 24 hr data sets cannot be considered representative of an entire season, sampling over a six-month period does provide an indication of long-term variations that may need to be considered in a future monitoring campaign, related to changes in ventilation, infiltration, and heating/air conditioning associated with changes in season.

2.1.2. Instrumentation

Table 1 provides details about the portable and non-portable real-time instruments that were employed in this study, including a particle counter (10-300 nm), a diffusion charger (DC) for total particle surface area, aerosol mass monitors for total mass concentrations and mass size distribution, plus a scanning mobility particle sizer (SMPS)

combined with an aerodynamic particle sizer (APS) for assessing particle number size distributions from the nano to coarse aerosol size ranges. These are all direct-reading instruments which monitor aerosols continuously with sampling intervals of 10 min for the TSI SMPS and APS, 1 min for the TSI DustTrak, 3 sec for the NanoTracer and 1 sec for the TSI 3786 CPC.

To prepare for the present study, all instrument units were either sent to the manufacturers for calibration or calibrated on-site according to manufacturers' recommended procedures. An instrument comparison study was also performed in the full-scale chamber using sodium chloride aerosol [37] to investigate consistency amongst the various particle counters before initiation of monitoring. Strong correlations were confirmed (e.g., $R^2 \geq 0.94$ for NanoTracer vs. TSI 3787 CPC and NanoTracer vs. TSI P-Trak CPC [37]).

2.1.3. Sampling locations

Table 2 provides sampling dates and descriptions of the six locations within a single federal government building in Ottawa, Canada. All locations are served by a heating, ventilation and air-conditioning (HVAC) system with outdoor air entrained and filtered into a central air handling unit and delivered to each location through ventilation ducting. Rooms 1 and 2 (Rm1 and Rm2) are both positively pressurized laboratories with their own air-conditioning units as required by the analytical instruments used in these rooms. Rm1 has dedicated HEPA filtration of supply air, while Rm2 does not (Table 2). The corridor (Cor) receives air flow from laboratories under positive pressure. Direct

exposure to outdoor air and motor vehicle particulate sources at the receiving/delivery area (R/D) location is likely due to its proximity to a garage-scale shipping entrance and another door for occupant entry. Rm3 has negative pressure relative to the corridor and is thus influenced by corridor air when the door is opened and via door leakage.

2.1.4. Experimental set-up

Background monitoring in Rooms 1-4 was conducted with all doors closed and the instrumentation placed in the center of each room, and with the air sampling inlets set at a height of 1.15m to represent the breathing zone of a seated office worker. For the corridor (Cor) and receiving/delivery area (R/D) locations, the sampling inlet was placed at a height of 1.65m to represent the breathing zone of standing or walking occupants.

2.2. Point source study

2.2.1. Study design

Laser printers were selected as a “point source” of engineered nanoparticles for comparisons with background measurements in this study, based on previous studies [5,17,34-36] which indicated that laser printers are a common source of NPs in the workplace. Two printer models that have been previously characterized [35] as high emitting printers, HP LaserJet 4200dtn and 4250dtn, were selected as emission sources in this study.

2.2.2. Sampling site

The printer emission experiment was performed in the National Research Council of Canada (NRC, Ottawa, Canada) full-scale stainless steel test chamber (55m³, internal dimensions: 5 × 4 × 2.75m) [38], which has a dedicated HVAC system including charcoal and HEPA filters. This facility controls and records complete test conditions including temperature, humidity, air flow rate and pressure at specified locations in and around the chamber. The full-scale chamber was used to ensure that the nanoparticles being characterized were emitted from the printer alone.

2.2.3. Experimental set-up

The NanoTracer and TSI SMPS systems described previously (Table 1) were employed for characterizing particle number concentration and particle number size distribution. All air sampling lines for the instruments were set at a height of 1.15 m (as in the background study) at a distance of 0.5 m from the printed page discharge outlet of the tested printer. Continuous printing for 300 pages (about 9 min duration) using a standard achromatic test chart RALA00.PDF [39] and single page printing (about 20 sec duration) were employed for particle number size distribution measurement and the point source study, respectively. Background levels inside the full-scale chamber were recorded for a period of 1 hr before and after printer emission testing. (Existing guidance for exposure assessment of nano-objects in the workplace[14] recommends that background determination measurements cover a time period of typically at least 45 min). All chamber experiments were performed under the following conditions: temperature 22-24°C, humidity 43-45%, return air flow 35 ft³ min⁻¹ and exhaust air flow of 17.5 ft³ min⁻¹ resulting in a chamber air exchange rate of 0.54 h⁻¹.

3. Results and discussion

3.1. Background study

3.1.1. Average background concentrations in test building

Table 3 summarizes particle number, total surface area and total mass concentration averages for daytime (12 hr, 6:30 am – 6:30 pm), nighttime (12 hr, 6:30 pm – 6:30 am) and 24 hr time periods in six locations of the test building (described in Table 2). Particle counts were obtained using the NanoTracer (from 10 – 300 nm); surface areas were obtained using the DC2000CE (all particle sizes up to 10 μ m); and the total PM mass concentrations were obtained using the DustTrak DRX (all particle sizes up to 15 μ m).

Typical particle number concentrations (10 – 300 nm) for the ground floor of the test building are in the range of 2.0 – 2.4 $\times 10^3$ # cm⁻³ based on an overall average of all six locations (Table 3). These are comparable to reported background NP values for other indoor environments (2.4 $\times 10^3$ # cm⁻³) [40] and office workplaces (1.5 – 7.5 $\times 10^3$ # cm⁻³) [5], and are low compared to NP exposures from cooking ($\sim 5 \times 10^3$ – 2 $\times 10^5$ # cm⁻³), second-hand smoking ($\sim 1 \times 10^4$ # cm⁻³), and average outdoor ambient background concentrations (8 $\times 10^3$ # cm⁻³) [40].

Background total surface area concentrations during the day and night in the six locations averaged 10.1 μ m² cm⁻³ and 8.6 μ m² cm⁻³ respectively (Table 3). Again, these values are low compared to outdoor ambient particle surface areas reported for an urban background site (50 – 70 μ m² cm⁻³) and an outdoor site near a freeway (100 – 150 μ m² cm⁻³) [41],

and much lower than values reported in a residential kitchen during cooking activities ($135 - 2000 \mu\text{m}^2 \text{cm}^{-3}$), inside an automotive engine plant ($250 - 2000 \mu\text{m}^2 \text{cm}^{-3}$) [23] and in a pizzeria ($200 - 20000 \mu\text{m}^2 \text{cm}^{-3}$) [6].

Background measurements of total PM mass concentrations averaged $8.5 \mu\text{g m}^{-3}$ for the six locations (Table 3). The corresponding PM_{10} and $\text{PM}_{2.5}$ averages were $5.5 \mu\text{g m}^{-3}$ and $5.6 \mu\text{g m}^{-3}$, respectively (not shown in Table 3), which were 10-20 times lower than PM_{10} or $\text{PM}_{2.5}$ levels reported for indoor environments with cooking sources [6, 42]. In summary, daytime averages exceeded nighttime averages for all metrics, notably total PM which decreased to $4.4 \mu\text{g m}^{-3}$ at night (Table 3).

3.1.2. Number size distribution

In the present study, five of the six investigated locations displayed bimodal distributions in the background signal (in Rm1 background number concentrations were too low to reliably identify modes; see Tables 4 and 5). Figure 1 provides an example of the bimodal number size distribution of the background signal (Rm2), with maxima at 27 nm and 98 nm, respectively. Bimodal size distributions were previously reported for background aerosol distributions in an indoor residential environment [43] with maxima at about 20 nm and 80 nm, and in a nanomaterial production facility [44] with maxima at 15 nm and 37 nm.

Table 4 summarizes the bimodal peak locations and peak heights in the different locations, and shows that the bimodal maxima vary from day to night, with daytime peak

values being generally higher than night time peak values. Higher values during the day are related to increased human activity and equipment usage during working hours, consistent with the well-documented “personal cloud” effect [45]. Table 4 also indicates large spatial variability, particularly in the first peak of the bimodal background signal which varies by more than an order of magnitude from Rm4 (3,700 at 33 nm) to the R/D location (89,000 at 30 nm) during the day. The origin of the bimodal size distributions could be partly explained by the nucleation of new particles leading to the first peak in the size distribution. Ageing processes then lead to the second peak, which is the accumulation mode. This might be the reason for the much higher peak at 30 nm in the R/D area (e.g. due to vehicle emissions).

Table 5 provides additional information about NP size distributions at different locations. Size distributions in the fine (100 – 1000 nm) and coarse (1 – 20 µm) particle ranges were also recorded to complete the background size spectra. Data provided include the daytime and night time averages for three nano-specific ranges (10-20 nm, 20-50 nm and 50-100 nm), two fine size ranges (100-500 nm, 500-1000 nm), and three coarse size ranges (1000-5000 nm, 5000-10000 nm and 10000-20000 nm). Note that the NPs (sum of the three nano-specific ranges) contribute 53% - 93% of the total indoor background particle number concentrations, while very fine (100 – 500 nm) and fine particle ranges (500 – 1000 nm) make smaller contributions: 5% – 39% and 1.4% – 15%, respectively (Table 5). Minor numbers of coarse particles from 1000 – 5000 nm were detected in indoor room environments, contributing <0.05% – 0.4% and <0.05% – 1.1% for day and night time, respectively. Particles larger than 5000 nm were negligible (< 0.01%; Table5). With respect to day-to-night variations, NPs (<100 nm) contribute 61%- 89% during the

day and 50 %– 76 % at night, respectively. Thus it can be concluded that particles in the nano size range dominate the indoor background aerosol when particle number concentrations are used as the metric.

3.1.3. Mass size distribution

Particle mass distribution data from PM_1 to $PM_{2.5}$, RESP (defined by TSI as PM_4) and PM_{10} (monitored using TSI DustTrak DRX; listed in Table 6) complete the picture provided by the above particle number concentration trends. Although PM_1 almost totally dominates the background particle mass at night (about 96%), it accounts for only about 78% during the day (Table 6). The difference in PM_1 between day and night is probably caused by the daytime increase in human activity/equipment usage which is accompanied by a larger contribution of coarser particles (22%) to the background particle mass.

Due to the limitations of the direct-reading mass measurement instruments, the precise contribution of NPs (<100 nm) to the total background mass concentration is unknown. Previous work using filter-based gravimetric methods in Rm2 showed that, of the total particle mass ($16 \mu\text{g m}^{-3}$), fine and ultrafine particles (10-560 nm) contributed 73% and coarse particles (1-10 μm) contributed 27% [17, 25, 46].

3.1.4. Spatial and temporal variations

The 24-hour average background particle number, surface area and mass concentrations vary widely amongst the six sampling locations (Table 7). The particle number concentration is a sensitive metric for monitoring spatial changes, exhibiting variations

exceeding one order of magnitude (from 2.6×10^2 to 6.3×10^3 #cm⁻³). Surface area varies by about an order of magnitude, and mass concentrations vary by three orders of magnitude from location to location within the same building (Table 7).

Variations of particle number concentrations in spring sampling versus winter sampling are shown in Fig.2a for daytime and Fig.2b for night. Although day and night trends are similar, number concentrations at night are generally lower than daytime concentrations, especially in spring at locations R/D and Rm3. R/D is a busy location during the day (Fig.2a) with frequent human activities that increase infiltration of outdoor air (receiving/delivering from a sliding garage door, and entry and exit of personnel from a regular entrance door). The corresponding night time value for R/D is much lower (Fig.2b) when such activities are at minimum. The difference between day and night in this area is a good example of the influence of human activities and outdoor air infiltration on indoor NP background values.

Figure 2 shows that particle number concentrations in spring were higher than in winter (Spring > Winter) for Rm3, Rm4 and R/D. However, the reverse trend (Spring ≤ Winter) was observed for Rm1, Rm2 and Cor (Figure 2). Researchers have reported [5, 40] that indoor particle number concentrations are usually directly related to outdoor particle number concentration, and that outdoor concentrations during winter are generally lower [47]. This reported seasonal trend (Spring > Winter) is most reflected by Rm3, Rm4 and R/D as indicated in Fig.2, suggesting that these areas are most influenced by outdoor air. The observation of a reverse trend (Spring ≤ Winter) for Rm1, Rm2 and Cor reflects the influence of environmental controls in the two positive pressure labs (Rm1 and Rm2) and

in the corridor area receiving the lab air (Cor). Particle number concentrations at these locations are more strongly influenced by the air handling systems within the building, and in the case of Rm1 (HEPA system in ceiling) diurnal and seasonal change is minimal.

Figures 3 and 4 illustrate temporal and spatial variations in surface area and mass, respectively, monitored simultaneously with particle number (Fig.2) at the same six locations. Similar to Fig.2, surface area values are 3 – 7 times lower in winter than in spring for Rm3, Rm4 and R/D, with values for R/D as high as $22.9 \mu\text{m}^2 \text{cm}^{-3}$ during the day and $17.2 \mu\text{m}^2 \text{cm}^{-3}$ at night. Figure 4 shows that spatial and seasonal variations of PM_{10} (Figs.4a and 4b) and total PM (Figs.4c and 4d) bear similarities to the trends shown in Fig.2 and Fig.3.

These results indicate that average values and standard deviations of background NP concentrations in the study building are dependent upon such factors as diurnal and seasonal variations, proximity to building entranceways such as the receiving area and loading dock, the degree of environmental controls in different workplace locations (e.g. laboratories versus office areas), and human activities. It is important to understand these background characteristics in order to select an appropriate exposure assessment approach that will be able to distinguish releases of engineered nano-objects from background. As indicated in CSA (2012) guidance [15], such indoor environmental factors need to be considered when making background corrections in exposure assessments.

Based on observations for background number, surface area and mass (Figs. 2-4), the lowest and least variable values were observed in Rm1, which can be attributed to the greater environmental controls in this room. The evidence of time trends observed in other locations (e.g. the increase from winter to spring in Rm3 and Rm4) indicates that an evaluation based only on mean and standard deviation is not sufficient and that time series data should be provided as well. Average and standard deviation values for particle number concentrations (e.g., Tables 3 and 7) do not provide adequate information about temporal trends in variability. Figure 5 provides an example of a time series over a 24 hr period in Rm2, a location that was characterized in Fig.2 as being one of the least-variable locations. Despite being a positive pressure lab with environmental controls, Rm2 displays large diurnal variability and even successive midnight values show a three-fold variation (from 900 to 300 # cm⁻³; Fig.5). Surface area and mass (total PM) monitored simultaneously in the same location also displayed large diurnal variability (from 3 to 37 μm²cm⁻³ and from 8 to 25 μg m⁻³, respectively; not shown here). No occupants used the room during the monitoring process, and there were no other identifiable causes for the variations. Such complicated and unpredictable temporal variations indicate the value of collecting time series data to characterize background nanoparticles in exposure assessments.

3.2. Point source study: Distinguishing point source emissions (printer example) from background

Figure 6 shows the particle number size distribution of emissions during continuous printing by a laser printer in the full scale chamber. The recorded particle size distribution ranges from 40 - 280 nm (mainly within 45 – 180 nm) with modes at 79 nm and 109 nm, respectively. Note that Fig.6 represents only a “snapshot” of the size distribution which continuously changes due to particle coagulation and loss processes. Also, based on previous work [35], it should be noted that the printer model employed in this study is classified as a high emitting printer and that the magnitude of printer emissions varies according to make and model. Therefore these results cannot be generalized to other printer emissions.

Figure 7 shows the time profile for emissions from printing a single page using the same laser printer, quantified using the NanoTracer. (It was not possible to capture the particle size distribution of a single print emission due to the longer response time of the SMPS used in this study.) The NanoTracer data in Fig. 7 were collected in the chamber where the background particle count averaged 209 \# cm^{-3} (compared to the much higher background values in the real-world example shown in Figure 5; $1000 - 2000 \text{ \# cm}^{-3}$ during daytime).

Figure 7 indicates that, inside the chamber, the peak number concentration is about 400 times higher than the chamber background, showing clear distinguishability between the

tested printer emissions and background signals. Had the single-page printer emission experiment (Fig.7) been conducted in the non-HEPA laboratory background environment shown in Fig.5, the emission peak to background peak (e-peak/b-peak) ratio would be 54, large enough to distinguish source emissions from the background. Actually, the e-peak/b-peak ratios are at least one to two orders of magnitude in five out of the six tested locations, i.e. 134 \times , 54 \times , 41 \times , 19 \times , and 16 \times for Rm1, Rm2, Cor, Rm3, and Rm4, respectively (referring to the peak values listed in Table 7). The e-peak/b-peak ratio is about 6 \times in the R/D location. Thus, even taking into account the complex temporal variations, it would be possible to distinguish this printer emission from the background at each of the six locations due to the large e-peak/b-peak ratios.

4. Conclusions

This study provided information about the variability of the background aerosol that will assist in designing real-time measurement strategies (e.g., duration and frequency of monitoring, monitoring locations) for future assessments of exposure to airborne engineered NPs. It shows that, depending on location in the building, time series data may be required to characterize diurnal variations and longer-term trends (such as seasonal variations) in addition to shorter-term average and standard deviation values.

Simultaneous monitoring of particle size, number, mass and surface area using multiple direct-reading instruments (e.g., SMPS, CPC, APS, DC and mass monitors) provides information about the full size range of background aerosols (nano- to micron-scale) and

is a recommended strategy for monitoring both NP background and point source exposures.

The particle number size distribution results show that incidental NPs are a major contributor to the background, accounting for 53% – 93% of the total number concentrations. The size distributions at the tested workplaces were bimodal with the first mode located within the 21 – 79 nm range and second mode within the 70 –136 nm range, depending on location.

The point source study indicates some limitations of the existing direct-reading instrumentation. First, the response time of the SMPS is too slow to capture rapid particle size distribution changes in NP emissions, such as laser printer emissions when printing a single page. The time resolution of particle counters (e.g. CPC and NanoTracer) is sufficient to monitor rapid changes in total particle number concentrations (as shown in Fig. 7). Therefore, both types of instruments are recommended for emission monitoring as they provide complementary information. Second, the direct-reading instruments used in this study do not have the capacity to distinguish amongst different types of particles and therefore cannot directly identify emission sources. In this study, an older model laser printer emitted NPs at peak concentrations 6 to 134 times background in the studied locations and thus were distinguishable on the basis of number concentration. However, lower emissions from more recent printers are likely to be indistinguishable, requiring off-line chemical analysis and/or electron microscopy to characterize particle components as necessary to identify sources.

Acknowledgments

We gratefully acknowledge the assistance of F. Muhammad, C. Levesque and L. Lavigne-Brunette. We are grateful for constructive comments and suggestions from two anonymous reviewers, and for helpful reviews of an early draft version by Drs. I. Jayawardene and L. Avramescu. This project was funded by Health Canada's Chemicals Management Plan, Clean Air Regulatory Agenda, and Environmental Health Sciences Research Bureau.

References

- 1 D. Brouwer, M. Berges, M. A. Virji, W. Fransman, D. Bello, L. Hodson, S. Gabriel, and E. Tielemans, Harmonization of measurement strategies for exposure to manufactured nano-objects; Report of a workshop, *Ann. Occup. Hyg.*, 2012, **56**, 1-9.
- 2 T.A.J. Kuhlbusch, C. Asbach, H. Fissan, D. Göhler and M. Stintz., Nanoparticle exposure at nanotechnology workplaces: A review. *Particle and Fibre Toxicology*, 2011, **8**, 1-18. <http://www.particleandfibretoxicology.com/content/8/1/22>.
- 3 M. Methner, L. Hodson and C. Geraci, Nanoparticle emission assessment technique (NEAT) for the identification and measurement of potential inhalation exposure to engineered nanomaterials — Part A, *J. Occup. Environ. Hyg.*, 2009, **7**, 127–132.
- 4 ISO (International Organization for Standardization), Nanotechnologies: terminology and definitions for nano-objects—nanoparticle, nanofibre and nanoplate, *ISO/TS 27687,2008*, Geneva, Switzerland.
- 5 P. McGarry, L. Morawska, R. Jayaratne, M. Falk, Q. Tran, and H. Wang, Exposure to particles from laser printers operating within office workplaces, *Environ. Sci. Technol.*, 2011, **45**, 6444-52.
- 6 G. Buonanno, L. Morawska, L. Stabile and A. Viola, Exposure to particle number, surface area and PM concentrations in pizzerias, *Atmos. Environ.*, 2010, **44**, 3963-3969.
- 7 L. A. Wallace, F. Wang, C. Howard-Reed and A. Persily, Contribution of gas and electric stoves to residential ultrafine particle concentrations between 2 nm and 64 nm: size distributions and emissions and coagulation rates, *Environ. Sci. Technol.*, 2008, **42**, 8641-8647.
- 8 B. Nowack, and T. D. Bucheli, Occurrence, behavior and effects of nanoparticles in the environment, *Environ. Pollut.*, 2007, **150**, 5-22.
- 9 J. Niu, P. E. Rasmussen, N.M. Hassan and R. Vincent, Concentration distribution and bioaccessibility of trace elements in nano and fine urban airborne particulate matter: influence of particle size, *Water Air Soil Pollut.*, 2010, **213**, 211–225.
- 10 T. A. J. Kuhlbusch, S. Neumann and H. Fissan, Number size distribution, mass concentration, and particle composition of PM₁, PM_{2.5}, and PM₁₀ in bag filling areas of carbon black production. *J. Occup. Environ. Hyg.*, 2004, **1**, 660–671.
- 11 NIOSH, Approaches to Safe Nanotechnology: Managing the Health and Safety Concerns Associated with Engineered Nanomaterials, *DHHS (NIOSH) Publication No. 2009–125*, March 2009.
- 12 D. H. Brouwer, J. H. J. Gijsbers and M. W. M. Lurvink, Personal exposure to ultrafine particles in the workplace: exploring sampling techniques and strategies, *Ann Occup. Hyg.*, 2004, **48**, 439–453.
- 13 M. Methner, L. Hodson, A. Dames and C. Geraci, Nanoparticle emission assessment technique (NEAT) for the identification and measurement of potential inhalation exposure to engineered nanomaterials — Part B: results from 12 field studies. *J. Occup. Environ. Hyg.*, 2009, **7**, 163–176.

- 14 C. Asbach, T.A.J. Kuhlbusch, H. Kaminski, B. Stahlmecke, S. Plitzko, U. Götz, M. Voetz, H. J. Kiesling and D. Dahmann, NanoGEM Standard Operation Procedures for assessing exposure to nanomaterials, following a tiered approach, 2012.
http://www.nanogem.de/cms/nanogem/upload/Veroeffentlichungen/nanoGEM_SOPs_Tiered_Approach.pdf
- 15 CSA Group, Nanotechnologies — Exposure control program for engineered nanomaterials in occupational settings, *Z12885-12*, Sept. 2012.
- 16 OECD 2009 Emission assessment for the identification of sources and release of airborne manufactured nanomaterials in the workplace: compilation of existing guidance ENV/JM/MONO 16.
- 17 J. Niu, P. E. Rasmussen and F. Muhammad, Characterization of airborne nanoparticles using a combination of in situ direct-reading and filter-based mass measurement strategies, *7th International Conference on the Environmental Effects of Nanoparticles and Nanomaterials*, P15. Banff, Alberta, Sept. 10-12, 2012.
- 18 M. M. Dahm, D. E. Evans, M. K. Schubauer-Berigan, M. E. Birch and J. A. Deddens, Occupational exposure assessment in carbon nanotube and nanofiber primary and secondary manufacturers: mobile direct-reading sampling, *Ann. Occup. Hyg.*, 2013, **57**, 328–344.
- 19 S. Y. Paik, D. M. Zalk and P. Swuste, Application of a pilot control banding tool for risk level assessment and control of nanoparticle exposures, *Ann. Occup. Hyg.*, 2008, **52**, 419-428.
- 20 A. D. Maynard and R. J. Aitken, Assessing exposure to airborne nanomaterials: Current abilities and future requirements, *Nanotoxicology*, 2007, **1**, 26-41.
- 21 R. Duffin, C. L. Tran, A. Clouter, D. M. Brown, W. MacNee, V. Stone and K. Donaldson, The importance of surface area and specific reactivity in the acute pulmonary inflammatory response to particles, *Ann. Occup. Hyg.*, 2002, **46**, 242–245.
- 22 G. Oberdörster, J. Ferin and B. E. Lehnert, 1994. Correlation Between Particle-Size, in-Vivo Particle Persistence, and Lung Injury, *Environ. Health Perspect.*, 1994, **102**, 173-179.
- 23 W. A. Heitbrink, D. E. Evans, B. K. Ku, A. D. Maynard, T. J. Slavin and T. M. Peters, Relationships among particle number, surface area, and respirable mass concentrations in automotive engine manufacturing, *J. Occup. Environ. Hyg.*, 2008, **6**, 19-31.
- 24 J. Niu, P. E. Rasmussen, F. Muhammad, C. Levesque and M. Chénier, From micro to nano: Instrumentation for measurement of airborne particles in the workplace, *2011 Health Canada Science Forum*, J-1.44. Ottawa, Ontario, Nov. 7-8, 2011.
- 25 J. Niu, P. E. Rasmussen and B. G. Fraser, Characterization of nanoparticles in the indoor environment: Collection strategy, size distributions and element signatures, *2010 Health Canada Science Forum*, J-3.18, Ottawa, Ontario, Nov. 1-2, 2010.

- 26 G. Ramachandran, D. Paulsen, W. Watts and D. Kittelson, Mass, surface area and number metrics in diesel occupational exposure assessment, *J. Environ. Monit.*, 2005 **7**, 728-735.
- 27 F. E. Pfefferkorn, D. Bello, G. Haddad, J.-Y. Park, M. Powell, J. McCarthy, K. L. Bunker, A. Fehrenbacher, Y. Jeon, M. A. Virji, G. Gruetzmacher and M. D. Hoover, Characterization of exposures to airborne nanoscale particles during friction stir welding of aluminum, *Ann. Occup. Hyg.*, 2010, **54**, 486-503.
- 28 D. E. Evans, W. A. Heitbrink, T. J. Slavin and T. M. Peters, Ultrafine and respirable particles in an automotive grey iron foundry, *Ann. Occup. Hyg.*, 2008, **52**, 9–21.
- 29 W. A. Heitbrink, D. E. Evans, T. M. Peters and T. J. Slavin, The characterization and mapping of very fine particles in an engine machining and assembly facility, *J. Occup. Environ. Hyg.*, 2007, **4**, 341–351.
- 30 A. Elder, R. Gelein, V. Silva, T. Feikert, L. Opanashuk, J. Carter, R. Potter, A. Maynard, Y. Ito, J. Finkelstein and G. Oberdörster, Translocation of inhaled ultrafine manganese oxide particles to the central nervous system, *Environ. Health Perspect.*, 2006, **114**, 1172–1178.
- 31 A. Wiebel, R. Bouchet, F. Boulch and P. Knauth, The big problem of particle size: a comparison of methods for determination of particle size in nanocrystalline anatase powders, *Chem. Mater.*, 2005, **17**, 2378–2385.
- 32 P. E. Rasmussen, I. Jayawardene, D. Gardner, M. Chénier, L. Christine and J. Niu, Metal impurities provide useful tracers for identifying exposures to airborne single-wall carbon nanotubes released from work-related processes, *J. Phys.: Conference Series* 429(2013)012007. DOI: 10.1088/1742-6596/429/1/012007.
- 33 J. Niu, P. E. Rasmussen and M. Chénier, Ultrasonic dissolution for ICP-MS determination of trace elements in lightly loaded airborne PM filters, *Int. J. Environ. Anal. Chem.*, 2013, **93**, 661-678.
- 34 H. Destailats, R. L. Maddalena, B. C. Singer, A. T. Hodgson and T. E. McKone, Indoor pollutants emitted by office equipment: A review of reported data and information needs, *Atmos. Environ.*, 2008, **42**, 1371-88.
- 35 C. He, L. Morawska and L. Taplin, Particle emission characteristics of office printers, *Environ. Sci. Technol.*, 2007, **41**, 6039-45.
- 36 J. Niu, P. E. Rasmussen and B. G. Fraser, Exposure to nanoparticles and associated metals in the office environment: concentration distributions and laser printer emissions, *HECSB Science, Policy and Regulatory Symposium-2010*, Health Canada, Ottawa, Ontario, Canada, March 23, 2010.
- 37 J. Niu, P. E. Rasmussen, R. Magee and G. Nilsson, Monitoring strategy for characterization of airborne nanoparticles, Proceedings of NanoTech-Advanced Materials and Applications (NanoTech 2014), Washington DC, USA, June 15-18, 2014, MO4.025 (1) 495.
- 38 National Research Council Canada, Material Emissions Laboratory - Full-Scale Test Chamber, <http://archive.nrc-cnrc.gc.ca/eng/facilities/irc/full-scale-chamber.html>.

- 39 BAM Federal Institute for Materials Research and Testing, Germany. Achromatic test chart with area coverage 5% (900 kByte, 504 pages), Emissions from office equipment with print functions according to RAL-UZ122:2006-04.
<http://www.ps.bam.de/RALUZ122/RALA00.PDF>
- 40 L. Wallace and W. Ott, Personal exposure to ultrafine particles, *J. Expo. Sci. Environ. Epidemiol.*, 2011, **21**, 20-30.
- 41 L. Ntziachristos, A. Polidori, H. Phuleria, M. D. Geller and C. Sioutas, Application of a diffusion charger for the measurement of particle surface, *Aerosol Sci. Technol.*, 2007, **41**, 571-580.
- 42 G. Buonanno, L. Morawska and L. Stabile, Particle emission factors during cooking activities, *Atmos. Environ.*, 2009, **43**, 3235-3242.
- 43 Y. Zhu, W. C. Hinds, M. Krudysz, T. Kuhn, J. Froines and C. Sioutas, Penetration of freeway ultrafine particles into indoor environments, *Aerosol Sci.*, 2005, **36**, 303-322.
- 44 T. Tritscher, M. Beeston, A. F. Zerrath, S. Elzey, T. J. Krinke, E. Filimundi and O. F. Bischof, NanoScan SMPS – A novel, portable nanoparticle sizing and counting instrument, *J. Phys.: Conference Series*, 2013, **429**, 012061. doi:10.1088/1742-6596/429/1/012061.
- 45 USEPA, Review of the national ambient air quality standards for particulate matter: Policy Assessment of Scientific and Technique Information., *EPA-452/R-05-005a*, December 2005. Chapter 2.7, 2-68z69.
- 46 P. E. Rasmussen, J. Niu and H. D. Gardner, Characterization of airborne nanoparticles using filter-based methods: metals and gravimetric analysis. *Tri-National Workshop on Standards for Nanotechnology*, National Research Council, Ottawa, Canada. Feb 3-4, 2010. <http://www.reno.nrc.cnrc.gc.ca/eng/events/inms/2010/02/03/tri-national-workshop.html>.
- 47 C. O. Stanier, A. Y. Khlystov and S. N. Pandis, Ambient aerosol size distributions and number concentrations measured during the Pittsburgh air quality study (PAQS), *Atmos. Environ.*, 2004, **38**, 3275-84.

Captions for Tables and Figures

Table 1. Description of the direct-reading instruments employed in this study.

Table 2. Description of the background aerosol monitoring locations and sampling dates. All rooms have linoleum floors; occupants were prevented from entering during monitoring except for R/D and Cor. No room contained copiers or printers. Average temperature and humidity are 25.0 °C and 24.6% RH during spring and 23.2 °C and 9.6% RH in the winter.

Table 3. Average background particle number, surface area and total mass (PM₁₅) concentrations for spring sampling of the six monitoring locations, using the NanoTracer, EcoChem DC2000CE and DustTrak, respectively. Instrument details are provided in Table 1.

Table 4. Bimodal number concentrations measured from 10.6 – 495.8 nm using TSI SMPS at different indoor workplaces (winter sampling). Modes could not be identified in Rm1 due to low number concentrations.

Table 5. Day/night variations in particle size distributions collected by TSI SMPS and APS at different workplace locations in winter (daytime = 12 hr, night time = 12 hr). The % values = # in a range / # in total (10 nm to 20 µm).

Table 6. Average particle mass distributions collected by DustTrak from the six monitoring locations in the spring. RESP = PM₄.

Table 7. Room to room variations in particle number, surface area and particle mass concentrations measured by NanoTracer, DC2000CE and DustTrak, respectively. Averages are given for a 24 hr period; spring sampling.

Figure 1. Example of bimodal particle size distribution of the background signal monitored using TSI SMPS (Rm2 winter sample is shown here; see Table 4 for other locations).

Figure 2. Comparison of spatial variations of the background particle number concentrations using NanoTracer between spring (■) and winter (○) for day (a) and night (b).. Error bars = 1 std dev for 12 hr.

Figure 3. Comparison of spatial variations of the background active surface areas using DC2000CE between spring (■) and winter (○) for day (a) and night (b)..

Figure 4. Comparison of spatial variations of the background PM₁ (**a** and **b**) and the total mass (**c** and **d**) concentrations using DustTrak between spring (■) and winter (○) for day (**a** and **c**) and night (**b** and **d**)..

Figure 5. Diurnal variations of background particle number concentrations recorded using NanoTracer in Rm2 (spring sample; See Fig.3 for other locations and seasons).

Figure 6. Particle size distribution of emissions from the HP LaserJet model 4200dtn during continuous printing recorded in the full scale chamber using TSI SMPS.

Figure 7. Particle number concentrations emitted from a HP LaserJet model 4200dtn printer for a single printing recorded in the full scale chamber using NanoTracer in fast scan mode (data logging every 3s). Background average is 209 \# cm^{-3} .

Table 1

Instrument	Particulate analysis capability
Aerasense NanoTracer (Philips Electronics, Eindhoven, The Netherlands)	<ul style="list-style-type: none"> • Particle counter for size range 10 - 300 nm; monitors total particle number concentration; units $\#/cm^3$
TSI Model 3936 scanning mobility particle sizer (SMPS) (TSI Inc., St. Paul, MN, USA), including: <ul style="list-style-type: none"> • A model 3080 electrostatic classifier • A model 3081 long differential mobility analyzer (DMA) • A model 3786 ultrafine water-based CPC 	<ul style="list-style-type: none"> • Monitors particle number size distributions; units $dN/d\log D_p$ ($\#/cm^3$) • 64 channels • size range 10.6 - 495.8 nm
TSI Model 3321 aerodynamic particle sizer (APS) (TSI Inc., St. Paul, MN, USA)	<ul style="list-style-type: none"> • Monitors particle number size distributions; units $dN/d\log D_p$ ($\#/cm^3$) • 32 channels • size range 500 nm - 20 μm
EcoChem DC2000CE diffusion charger (DC) (EcoChem Analytics, League City, TX, USA)	<ul style="list-style-type: none"> • Measures particle surface area concentration (units $\mu m^2/cm^3$)
TSI DustTrak DRX Model 8533 (TSI Inc., St. Paul, MN, USA)	<ul style="list-style-type: none"> • Monitors total particle mass (units $\mu g/m^3$), corresponding to PM_{10}, $PM_{2.5}$, respirable (RESP = PM_4), PM_{10} and total PM (equal to PM_{15})

Table 2

Location	Dates sampled	Area (m ²)	Description
Rm1	May 08-10 Dec 03-07	22.0	Clean laboratory (HEPA system in ceiling) with benches and a sink lining walls.
Rm2	May 10-16 Nov 26-29	8.7	Regular laboratory (without HEPA) with laminar fumehood.
Cor	Apr 26-30 Nov 29 - Dec 03	160.4	A corridor (88.1 m long and 1.82 m wide)
Rm3	Apr 23-26 Dec 07-11	12.7	Combined office/laboratory environment.
Rm4	May 03-07 Jan 08-13	16.9	A storage room containing floor-to-ceiling shelving.
R/D	Apr 30 - May 03 Jan 02-04	90.5	A receiving and delivering area with loading dock and service entrance.

Rm - room; Cor - corridor; R/D- receiving and delivering area.

Table 3

	<u>Day (12 hr)</u>		<u>Night (12 hr)</u>		<u>24 hr</u>	
	Ave ^a	Stdev ^b	Ave	Stdev	Ave	Stdev
Number concentration (# cm ⁻³)	2.4 × 10 ³	5.1 × 10 ²	2.0 × 10 ³	4.8 × 10 ²	2.2 × 10 ³	5.1 × 10 ²
Total surface area concentration (μm ² cm ⁻³)	10.1	3.9	8.6	3.7	9.5	3.9
Total mass concentration (μg m ⁻³)	8.5	2.3	4.4	1.1	6.5	2.1

^a average values; ^b standard deviation.

Table 4

Location	Time	First peak		Second peak	
		Peak location (nm)	Peak height (dN/dlogD _p , # cm ⁻³)	Peak location (nm)	Peak height (dN/dlogD _p , # cm ⁻³)
Rm1	day	-	-	-	-
	night	-	-	-	-
Rm2	day	27	1.5 × 10³	98	1.4 × 10 ³
	night	19	2.7 × 10 ²	106	1.2 × 10³
Cor	day	79	3.7 × 10 ³	106	3.7 × 10 ³
	night	74	3.4 × 10 ³	106	3.7 × 10³
Rm3	day	29	1.2 × 10³	136	5.0 × 10 ²
	night	39	7.1 × 10²	136	5.0 × 10 ²
Rm4	day	33	3.7 × 10 ²	109	6.8 × 10²
	night	33	2.3 × 10³	109	5.9 × 10 ²
R/D	day	30	8.9 × 10³	71	5.8 × 10 ³
	night	21	1.8 × 10 ³	50	5.6 × 10³

Bold number indicates the modes with larger peak height values.

Table 5

Location / time	Nano particles						Fine particles						Coarse particles					
	10-20 nm C (# cm^{-3}) %	20-50 nm C (# cm^{-3}) %	50-100 nm C (# cm^{-3}) %	100-500 nm C (# cm^{-3}) %	500-1000 nm C (# cm^{-3}) %	1000-5000 nm C (# cm^{-3}) %	5000-10000 nm C (# cm^{-3}) %	10000-20000 nm C (# cm^{-3}) %	1000-5000 nm C (# cm^{-3}) %	5000-10000 nm C (# cm^{-3}) %	10000-20000 nm C (# cm^{-3}) %	10000-20000 nm C (# cm^{-3}) %	10000-20000 nm C (# cm^{-3}) %	10000-20000 nm C (# cm^{-3}) %	10000-20000 nm C (# cm^{-3}) %			
Rm1	day	7.6x10 ⁻²	4.4	5.2x10 ⁻¹	30.1	1.0x10⁰	58.5	8.6x10 ⁻²	5.0	2.9x10 ⁻²	1.7	5.1x10 ⁻³	0.3	0	0.0	0	0.0	
	night	4.0x10⁻¹	39.4	2.6x10 ⁻¹	25.6	2.5x10 ⁻¹	24.6	8.1x10 ⁻²	8.0	1.4x10 ⁻²	1.4	1.0x10 ⁻²	1.0	0	0.0	0	0.0	
Rm2	day	9.2x10 ⁻¹	8.3	4.7x10²	42.3	3.3x10 ²	29.7	1.1x10 ²	10.3	1.0x10 ²	9.2	2.9x10 ⁰	0.2	7.5x10 ⁻²	0.0	0	0.0	
	night	9.9x10 ⁻¹	9.2	3.4x10²	31.2	3.1x10 ²	28.4	2.2x10 ²	20.8	1.1x10 ²	10.3	1.1x10 ⁰	0.1	4.8x10 ⁻³	0.0	0	0.0	
Cor	day	2.5x10 ⁻¹	1.9	2.2x10 ²	16.7	4.5x10 ²	34.2	5.0x10²	38.1	1.2x10 ²	9.0	8.8x10 ⁻¹	0.1	5.0x10 ⁻³	0.0	0	0.0	
	night	1.7x10 ⁻¹	1.7	1.2x10 ²	12.0	3.9x10²	39.2	3.9x10²	39.2	7.8x10 ⁻¹	7.8	6.8x10 ⁻¹	0.1	2.5x10 ⁻³	0.0	0	0.0	
Rm3	day	5.3x10 ⁻²	23.2	1.1x10³	49.5	2.5x10 ²	11.0	2.7x10 ²	11.7	9.5x10 ⁻¹	4.2	9.5x10 ⁰	0.4	0	0.0	0	0.0	
	night	1.2x10 ⁻²	4.0	9.1x10²	29.2	7.0x10 ²	22.7	8.9x10 ⁻²	28.5	4.7x10 ⁻²	15.0	2.0x10 ⁰	0.6	8.1x10 ⁻³	0.0	0	0.0	
Rm4	day	5.0x10 ⁻²	13.1	1.5x10³	39.7	1.0x10 ³	27.2	6.3x10 ⁻²	16.6	1.3x10 ⁻²	3.4	1.6x10 ⁰	0.0	1.8x10 ⁻²	0.0	0	0.0	
	night	6.7x10 ⁻¹	1.9	1.1x10 ³	29.9	1.3x10³	37.3	9.0x10 ⁻²	25.3	2.0x10 ⁻²	5.6	1.0x10 ⁰	0.0	1.5x10 ⁻³	0.0	0	0.0	
R/D	day	8.1x10 ⁻²	8.1	4.2x10³	41.9	2.4x10 ³	24.2	1.6x10 ³	17.6	7.9x10 ⁻²	7.9	3.1x10 ⁻¹	0.3	7.8x10 ⁻¹	0.0	5.9x10 ⁻³	0.0	
	night	1.7x10 ⁻²	3.2	2.1x10³	40.0	1.9x10 ³	36.2	6.2x10 ⁻²	12.0	3.9x10 ⁻²	7.5	5.4x10 ⁻¹	1.1	2.8x10 ⁻²	0.0	0	0.0	

C - particle number concentration; Rm- room; R/D - receiving and delivering area; % - percentage of the total particle number concentration. The bold number indicates the main particle size distribution sections.

Table 6

Mass ($\mu\text{g m}^{-3}$)	Day (12 hr)			Night (12 hr)			24 hr		
	Ave ^a	Stdev ^b	% ^c	Ave	Stdev	%	Ave	Stdev	%
< PM ₁	5.55	1.13	78.4	4.21	0.90	95.7	4.88	1.26	85.5
PM ₁ → PM _{2.5}	0.08	0.02	1.1	0.04	0.01	0.9	0.06	0.02	1.0
PM _{2.5} → RESP	0.21	0.05	3.0	0.05	0.01	1.1	0.14	0.03	2.5
RESP → PM ₁₀	1.24	0.39	17.5	0.10	0.03	2.3	0.63	0.19	11.0

^a average values; ^b standard deviation; ^c percentages, calculated using PM₁₀ as the total.

Table 7

Location	Number (# cm ⁻³)			Surface area (µm ² cm ⁻³)			Mass (µg m ⁻³)		
	Mean*	stdev	Peak	Mean*	stdev	PM ₁ *	PM _{2.5} * stdev	PM ₁₀ * stdev	
Rm1	2.6 × 10 ²	1.7 × 10 ²	6.4 × 10 ²	2.1	1.9	0.02	0.13	0.02	0.13
Rm2	8.8 × 10 ²	2.6 × 10 ²	1.6 × 10 ³	5.1	2.6	2.75	0.62	2.82	0.64
Cor	8.8 × 10 ²	2.9 × 10 ²	2.1 × 10 ³	3.3	2.2	1.61	0.91	1.66	0.98
Rm3	2.2 × 10 ³	8.0 × 10 ²	4.6 × 10 ³	9.9	4.5	4.45	1.03	4.46	1.04
Rm4	3.2 × 10 ³	6.0 × 10 ²	5.5 × 10 ³	17.7	4.6	7.89	1.73	7.92	1.74
R/D	6.3 × 10 ³	1.7 × 10 ³	1.4 × 10 ⁴	20.1	6.6	11.68	6.92	11.95	7.13
								14.20	11.01

* - 24 hr average concentration; stdev- standard deviation; Rm- room; Cor- corridor and R/D- receiving and delivering area.

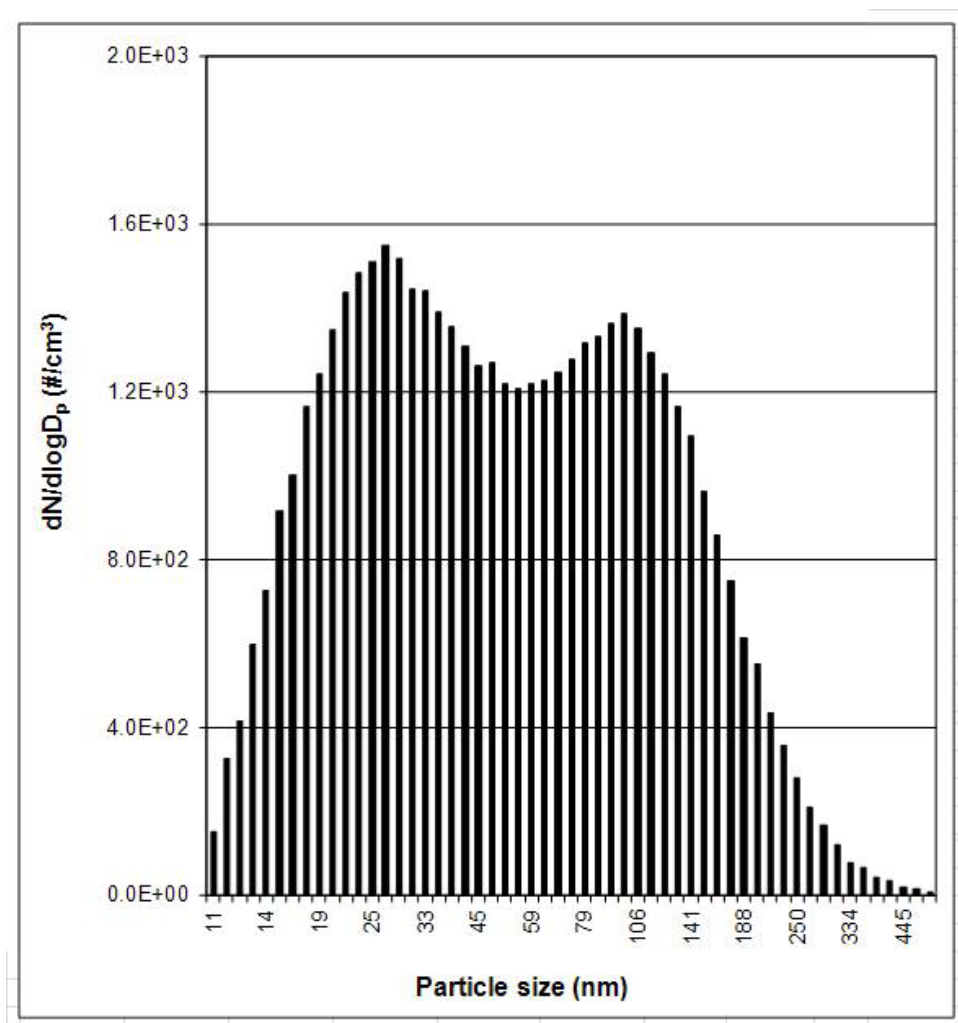


Fig.1

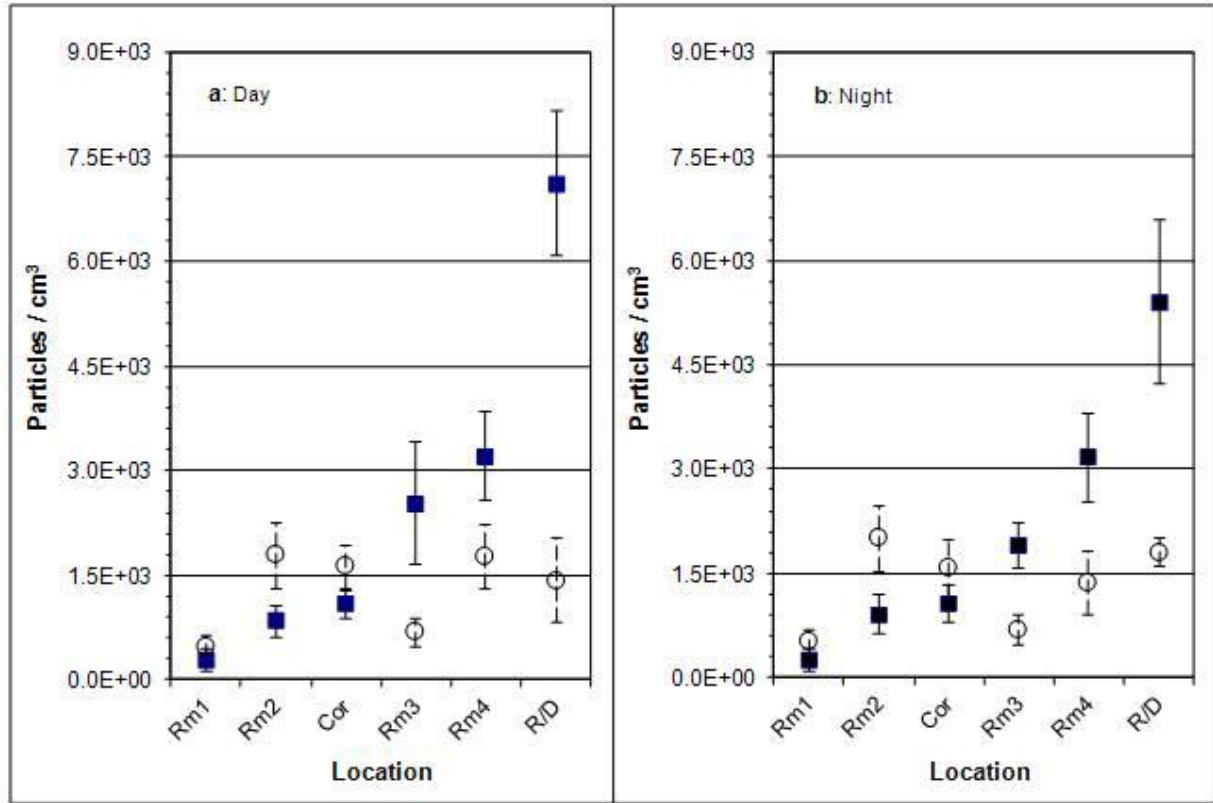


Fig.2

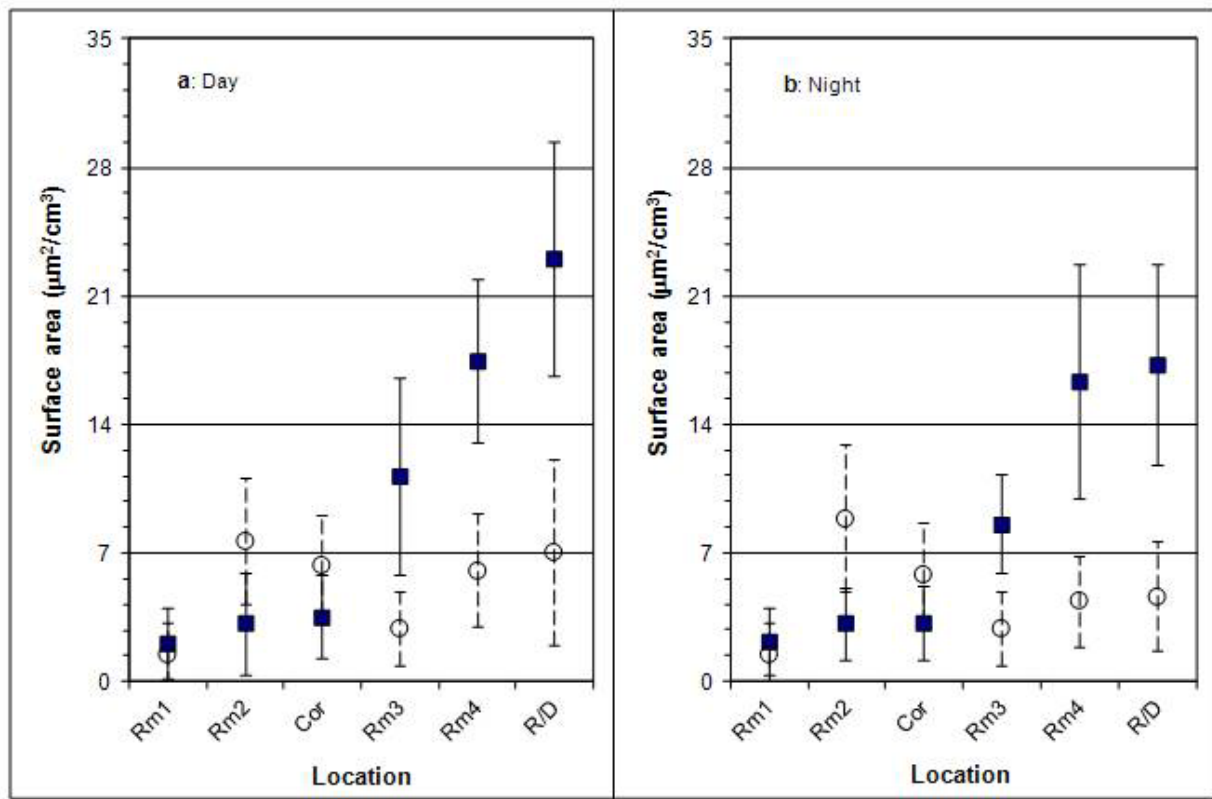


Fig.3

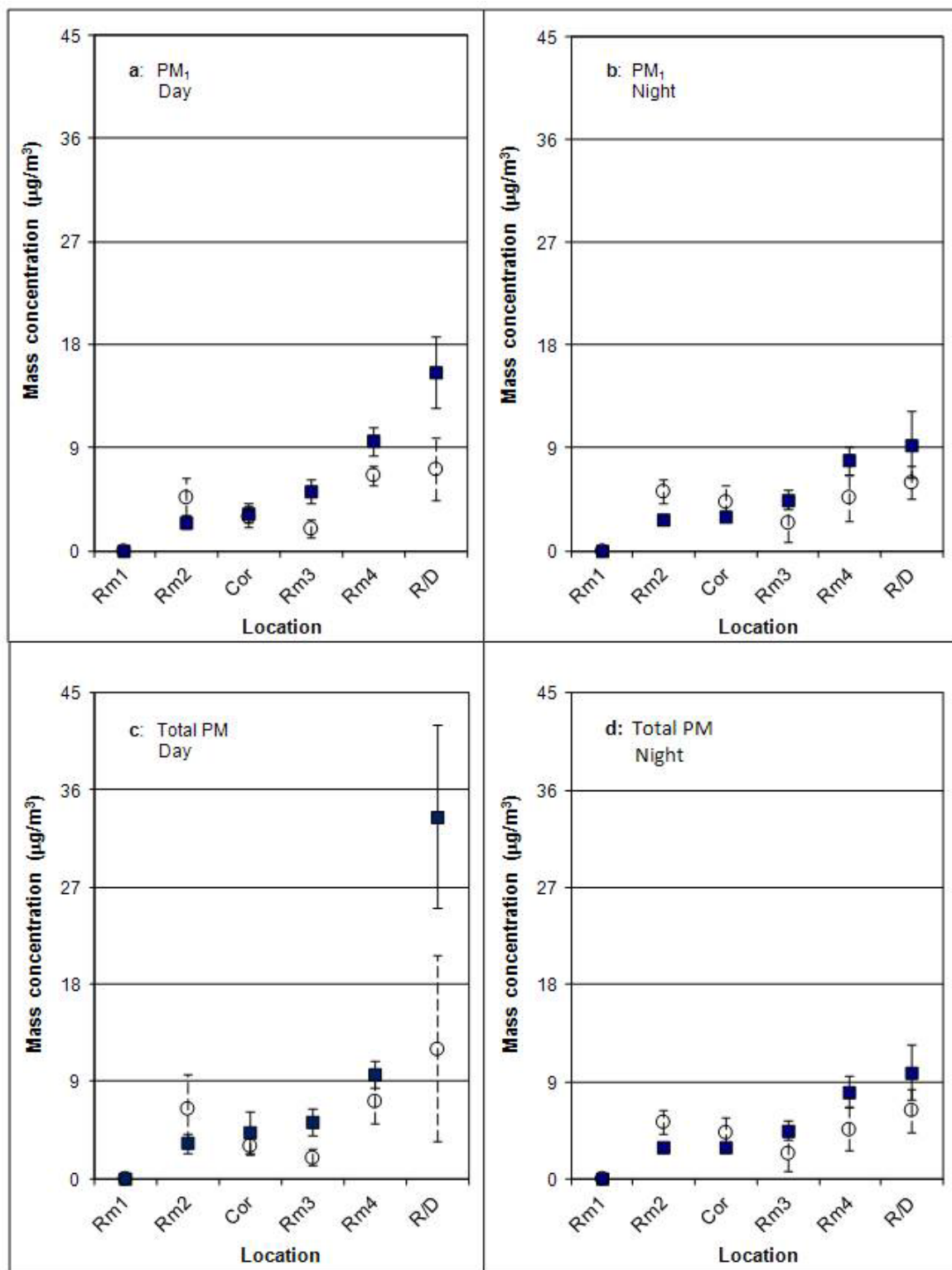


Fig.4

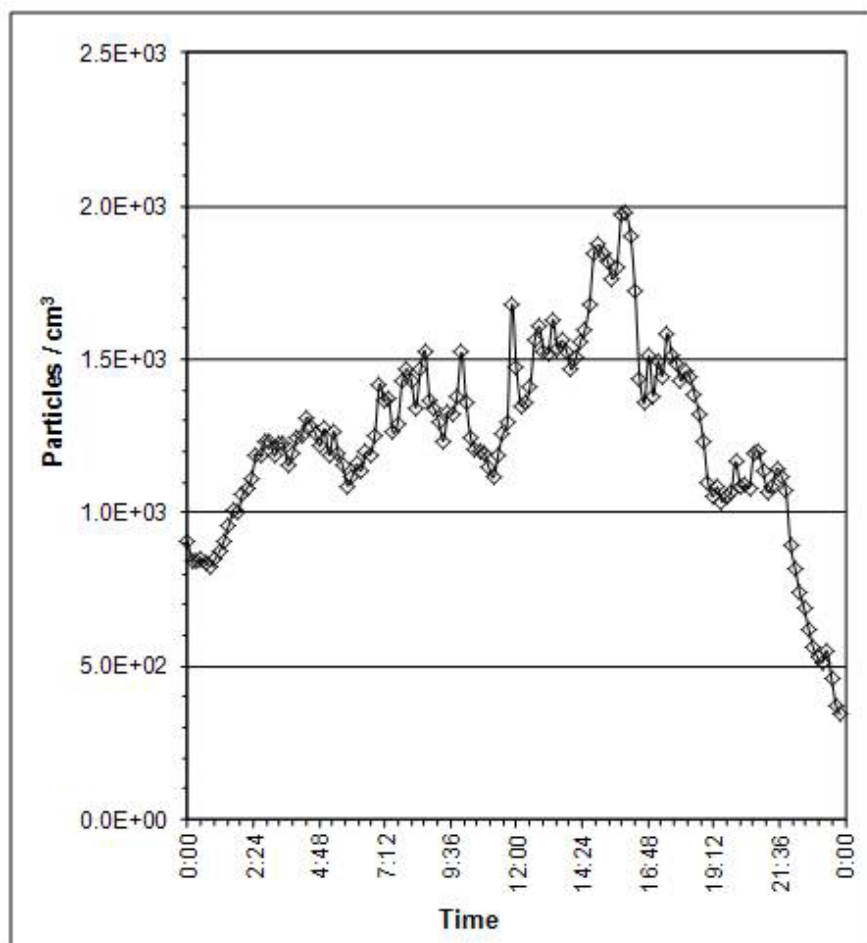


Fig.5

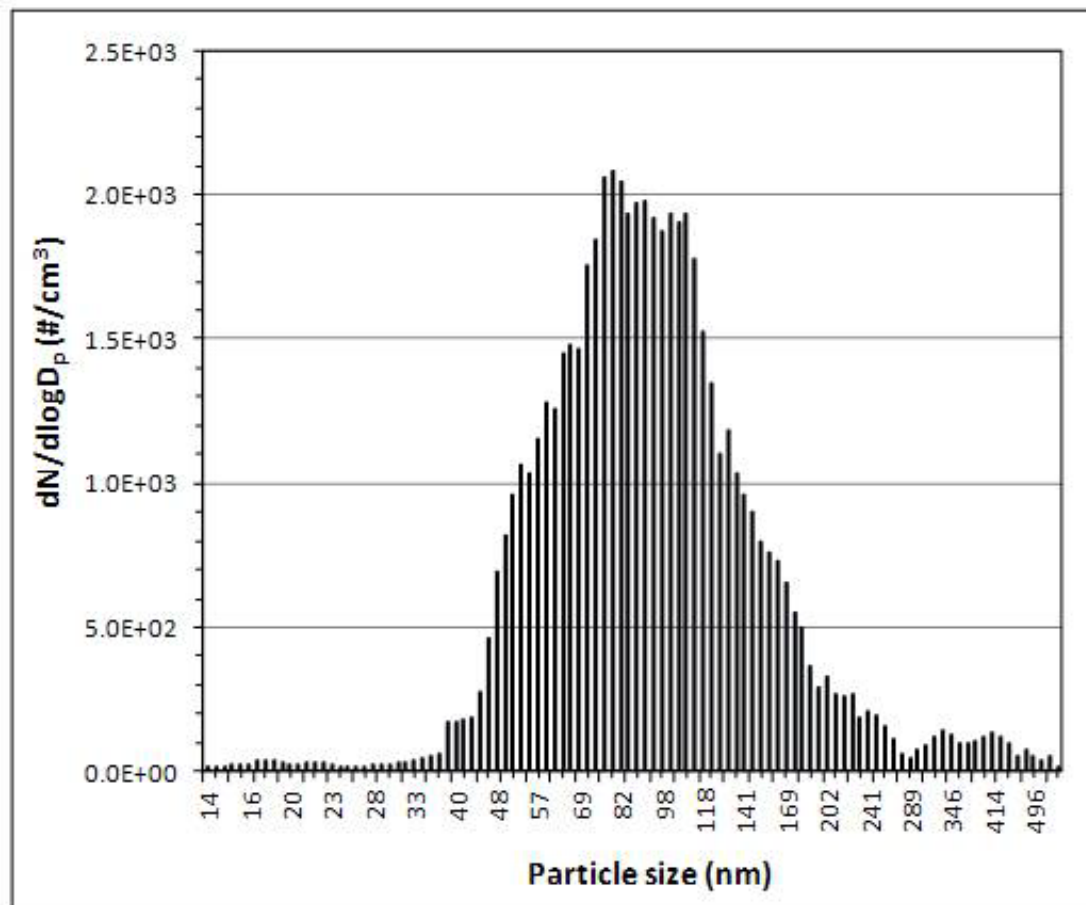


Fig.6

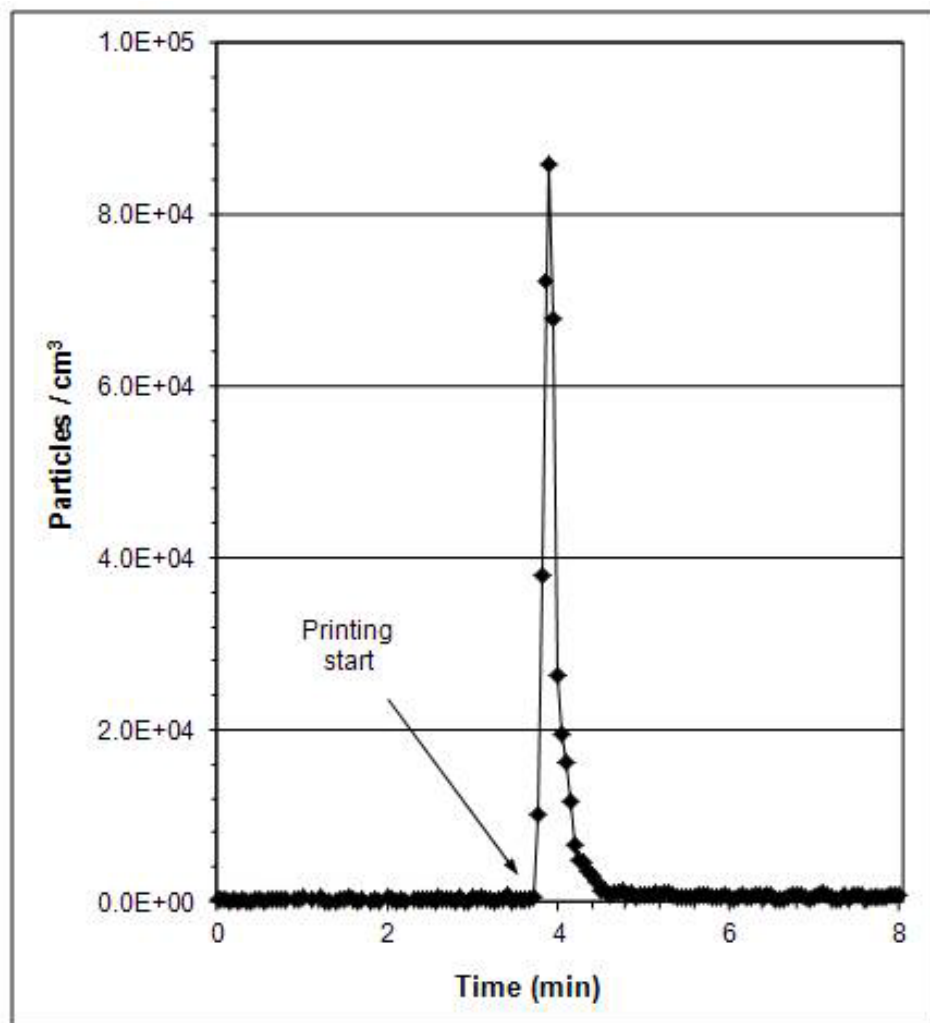


Fig.7